FATIGUE PROPERTIES OF NOTCHED SPECIMENS MADE OF FeP04 STEEL

D. ROZUMEK, Z. MARCINIAK

Opole University of Technology, Poland

Fatigue properties of the specimens with different notches made of FeP04 steel are presented. The specimens ware characterized by double symmetric lateral notches with a notch root radius ranging from ρ = 0.2 to 10 mm. The MTS 809 servo-hydraulic device was used for tests. All fatigue tests were performed under force control, by imposing a constant value of the nominal load ratio (R = 0) and a load amplitude P_a = 6 kN for the notch root ρ = 0.2 mm and 7 kN for the notch root ρ = 1.25; 2.5 and 10 mm. The test frequency varied from 13 and 15 Hz. During the tests under constant load fatigue weakening of the material and an increase in strain were observed.

Keywords: *fatigue, notch, strain, hysteresis loops.*

In the case of ductile cracking the specimen surface separation for pure metals occurs as a result of successive slip bands, and for technical alloys the cracking process starts with the harder components (non-metallic inclusions), creating voids thus causing the increasing damage to the process. In paper [1] ductile cast irons are characterized by high fatigue crack propagation resistance, although this property is still not widely investigated. In work [1], three different ferritic–pearlitic ductile cast irons, characterized by different ferrite/pearlite volume fractions and an austempered ductile cast iron were considered. Their fatigue crack propagation resistance was investigated in air by means of fatigue crack propagation tests according to ASTM E647 standard, considering three different stress ratios (R = 0.1; 0.5; 0.75). When fatigue crack is nucleated and propagates in the notch vicinity [2], the crack growth rate is generally higher than that expected by using the stress intensity factor concept. The current study attemptes to describe the crack growth at notches quantitatively with a detailed consideration of the material cyclic plasticity. The combined effect of notch plasticity and possible contact of cracked surface was responsible for the observed crack growth phenomenon near the notch. In paper [3], the influence of the notch radius on the crack growth rate under low- and high-cycle fatigue is discussed. Tests were carried out on the plates made of FeP04-UNI 8092 deep-drawing steel, weakened by symmetric lateral notches of varying acuity. It has been shown that the notch strongly influences the variation of ΔJ parameter values both globally and locally.

The aim of the paper is the determination of the fatigue properties of notched specimens made of FeP04 steel.

Material, properties and test stand. ***Static properties and fatigue tests of specimens.*** Tests were carried out on the plane specimens made of FeP04-UNI 8092 deep-drawing steel. Steel FeP04 was used for the load-bearing elements of construction vehicles. For static and fatigue tests, a Schenck PSA100 servo-hydraulic device was used. Coefficients of the Ramberg–Osgood equation describing the cyclic strain curve under tension-compression with $R_\varepsilon = -1$ (a Schenck extensometer was used with a gauge length equal to 25 mm) for FeP04 steel are the following [4]: the cyclic strength coefficient $K' = 838$ MPa, the cyclic strain hardening exponent $n' = 0.220$.

Corresponding author: D. ROZUMEK, e-mail: d.rozumek@po.opole.pl

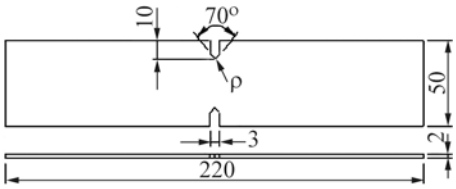

Fig. 1. Specimen for tests (dimensions in mm).

The specimens had double symmetric lateral notches with the notch root radii ranging from 0.2 to 10 mm (Fig. 1). The theoretical stress concentration factor in the specimen under tension K_t = 9.61; 4.30; 3.23 and 1.85 was estimated with use of the model presented in [5].

The surfaces of the specimens, w = 50 mm wide, had been accurately polished in order to make the cracks originated from the notch tip easily distinguishable. Test material is FeP04 steel (0.05 wt.% C, 0.30 Mn, 0.05 Si, 0.032 P, 0.02 S, 0.043 Al, 0.07 Cu, balance – Fe). The monotonic quasi-static tension properties of FeP04 steel are the following: yield stress σ_y = 210 MPa, ultimate stress σ_u = 330 MPa, Young's modulus E = 191 GPa, Poisson's ratio ν = 0.30. The MTS 809 servo-hydraulic device was used for tests. Both testing systems were equipped with a 100 kN load-cell. The stand MTS 809 contains a modulus which allows to perform tests under a given crack tip opening displacement δ. The modulus is included into the control panel. The displacement of a gage length was controlled. During fatigue crack growth, displacement was measured with an extensometer. For measurements the extensometer MTS was applied (gage length – 10 mm, model 632, 13F-20 manufactured by Systems Corporation Eden Prairie, USA). The test frequency ranged from 13 and 15 Hz. Crack initiation and propagation phases were observed on the specimen surface by means of a portable microscope having a magnification factor 20 times.

All fatigue tests were performed under force control, by imposing a constant value of the nominal load ratio ($R = \sigma_{min}/\sigma_{max} = 0$) and a load amplitude P_a = 6 kN (P_{max} = = 12 kN) for the notch root ρ = 0.2 mm and 7 kN (P_{max} = 14 kN) for the notch root ρ = 1.25, 2.5 and 10 mm (which corresponded to the nominal amplitude of normal net stresses σ_a = 100; 117 MPa before the crack initiation).

Results and discussion. ***Microstructure and fatigue crack path in FeP04 steel.*** Steel FeP04 can be easily subjected to cold working, it belongs to ferritic steels. Since the amount of carbon in ferrite is low, ferrite properties are very similar to the properties of pure iron α. The considered steel is applied for deep drawing. The material structures were tested on the metallographic specimens with the metallographic microscope magnifying from 50 till 2000 times. Fig. 2 shows microstructure of FeP04 steel, containing the ferrite (light) and numerous non-metallic inclusions. The structure exhibits a distinct rolling texture. Against a background of long ferrite grains there are numerous non-metallic inclusions visible, mainly chains of oxides about 1 μm (black). On the ferrite grain boundaries coalesced cementite can be seen in Fig. 2. In the material transcrystalline cracks through the grains of phase α are dominating, but cracks along the grain boundaries are also observed. The main cracks propagate in the direction perpendicular to the loading action, but secondary cracks are also visible. Fig. 3 presents the surface of a specimen tested under loading P_a = 7 kN and with the radius of the notch root ρ = 10 mm after N_f = 128700 cycles to failure. The development of cracks was observed under microscope at a magnification of 17 times. The initiation and growth of many cracks were observed at the notch tip. Due to high plasticity of the material ductile cracking is observed which is characterized by the presence of voids (black field around the notch – Fig. 3) after stratification of the material found on the crack paths. Stress concentration and intensification of the plastic flow occur around the voids.

The tests of fatigue crack growth in FeP04 steel subjected to tension were performed in the low and high cycles fatigue. During tests a number of cycles to the crack initiation N_i (i.e. to the moment of occurrence of a visible crack) was recorded, and the

fatigue crack lengths were measured. The cracks initiated [6] (minimal observable crack length about 0.1 to 0.2 mm) at the same time on the left and on the right sides of the notched specimen.

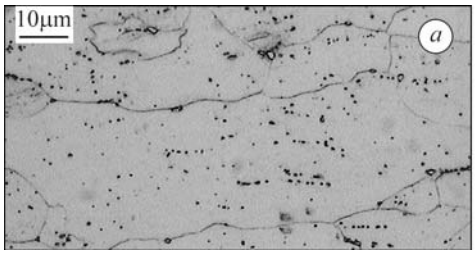

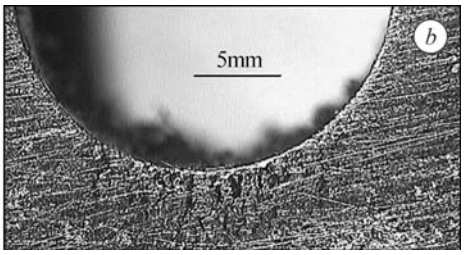

Fig. 2. Fig. 3.

Fig. 2. The FeP04 steel microstructure (grains phase α).

Fig. 3. The paths of cracks in the specimen with a notch radius ρ = 10 mm.

Fatigue characteristics of strain. Examples of the strain and force histories for the initial period (Fig. 4) and for the entire lifetime of the specimens (Fig. 5). Fig. 4 presents the sample characteristics of the strain and load for four types of notches ρ = = 0.2, 1.25; 2.5 and 10 mm. On the basis of Fig. 4*b* some anomalies can be stated in the strain history for the initial period of researches in comparison with other charts. This behavior could be caused by the material ratcheting.

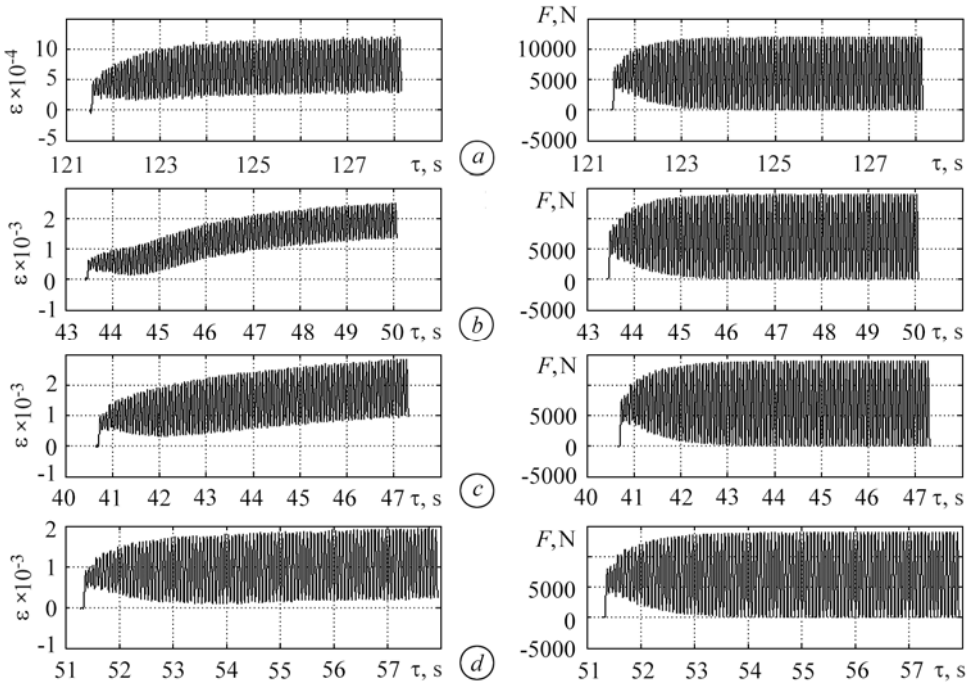

Fig. 4. Characteristics of strain, ε, and force, *F*, versus time, τ, for the initial period of researches and different notches: *a* – ρ = 0.2 mm; *b* – 1.25; *c* – 2.5; *d* – 10 mm.

The presented strain histories shown in Fig. 5 relate to different life obtained for different notches. For specimens with a notch ρ = 2.5 and 10 mm a slight increase in strain by about 85 and 95% life of the specimens can be seen. In contrast, for specimens with a notch ρ = 0.2 mm fluctuations were observed, and with a notch ρ = 1.25 mm the decrease in strain for about 120 s was observed. For the results shown in Fig. 5*a* in

low-cycles fatigue the initiation of cracks was observed in the initial period of researches. Fig. 5*b* shows that fatigue cracks initiation occurred after 8300 cycles due to the blunt notch radius ρ = 1.25 mm, although the crack growth took place under low-cycle fatigue. For the specimen in Fig. 5*d* the initiation of cracks occurred at the end of the specimen life. This is typical of high-cycles fatigue research. From the curves "strain vs time" reported in Fig. 5, it appears that after changing the notch root radii ρ from 0.2 to 10 mm fatigue life increases. It is evident that with the highest radius the initiation phase, which depends on the stress conditions at the notch tip, prevails.

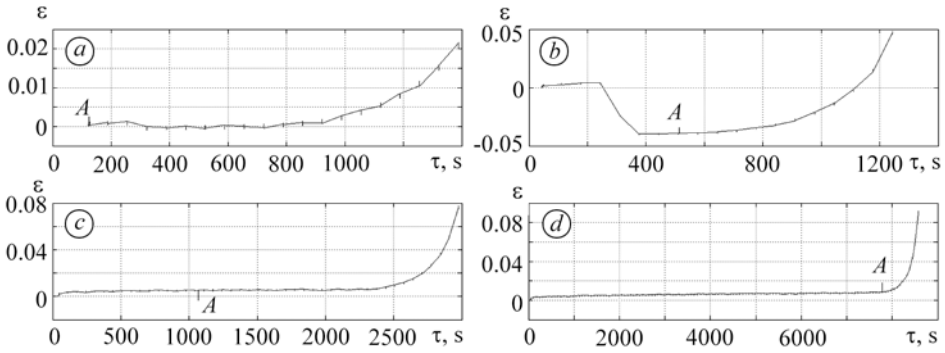

Fig. 5. Characteristics of strain, ε, versus time, τ, for the entire lifetime and different notches: *a* – ρ = 0.2 mm; *b* – 1.25; *c* – 2.5; *d* – 10 mm (*A* – crack initiation).

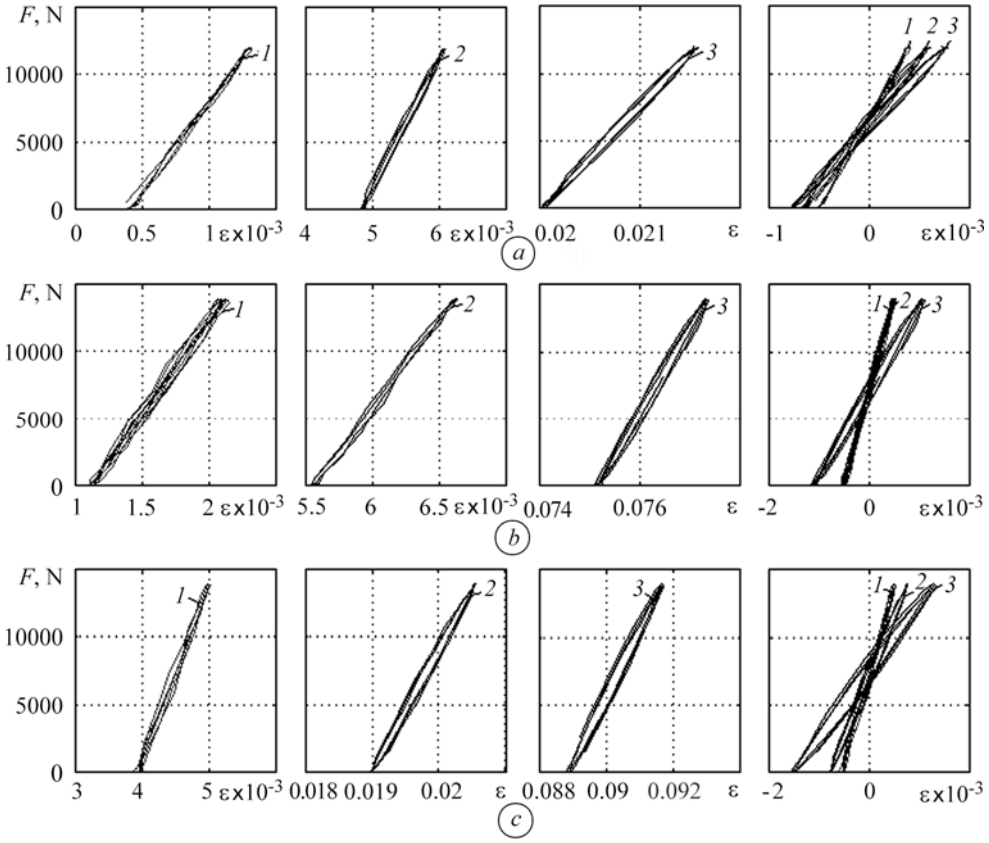

Fig. 6. Selected hysteresis loops at different times of tests for notches: *a* – ρ = 0.2 mm; *b* – 2.5; *c* – 10 mm.

Analysis. Fig. 6 shows the examples of hysteresis loops at different life times of the specimens with notches, where; *1* – the initial period of a specimen study (from Fig. 5),

2 – half of the specimen life and *3* – the final test period. Based on Fig. 6 it can be concluded that during the tests a marked increase in the total strain was noticed. Under test conditions for P_a = const the weakening of the material occurs when the strain amplitude increases with the increase of the hysteresis loop width. The fourth graph presented in Fig. 6 for different notches radii gives the hysteresis loops for periods *1*, *2* and *3*. From the graphs it can be concluded that for ρ = 0.2 and 10 mm increase in strain occurs evenly. However, for ρ = 2.5 mm it can be observed that in the late specimen life a sudden increase in strain takes place and the scope of these strains have the highest values.

Stresses at the notch root. In order to calculate the maximum stresses at the root notch the strain energy density models of Neuber [7], Molski–Glinka [8], Łagoda–Macha [9] were used. These models are based on the cyclic stress-strain curve and are presented by the following formulas:

$$W_N = \frac{\sigma_{\max}^2}{E} + \sigma_{\max}\left(\frac{\sigma_{\max}}{K'}\right)^{\frac{1}{n'}} \text{ (for Neuber)}, \tag{1}$$

$$W_{MG} = \frac{\sigma_{\max}^2}{2E} + \frac{\sigma_{\max}}{1+n'}\left(\frac{\sigma_{\max}}{K'}\right)^{\frac{1}{n'}} \text{ (for Molski–Glinka)}, \tag{2}$$

$$W_{LM} = \frac{\sigma_{\max}^2}{2E} + \frac{1-n'}{1+n'}\sigma_{\max}\left(\frac{\sigma_{\max}}{K'}\right)^{\frac{1}{n'}} \text{ (for Macha–Łagoda)}. \tag{3}$$

Above models are compared to the energy calculated using the nominal value of stresses and strains. The strain energy density value corresponding to the nominal stress was calculated by the equations:

$$W_n = \frac{(K_t\sigma_n)^2}{E}, \quad W_n = \frac{(K_f\sigma_n)^2}{E} \text{ (for Neuber)}, \tag{4}$$

$$W_n = \frac{(K_t\sigma_n)^2}{2E}, \quad W_n = \frac{(K_f\sigma_n)^2}{2E} \text{ (for Molski–Glinka and Macha–Łagoda)}, \tag{5}$$

where K_f is fatigue stress concentration factor.

The distribution of stresses in a notched specimen subjected to tension is shown in Fig. 7.

Fig. 7. Gradient stress in a notched tensile specimen.

Comparison of models (1)–(3) with equations (4) and (5) allowed to calculate the maximum stresses at the notch root. The results are shown in Tables 1 and 2.

Table 1. Dependences of σ_{max} versus K_t and strain energy density models

K_t	Model		
	Neuber	Molski–Glinka	Macha–Łagoda
	σ_{max}, MPa		
9.61	421	386	405
4.30	329	302	316
3.23	294	270	282

Table 2. Dependences of σ_{max} versus K_f and strain energy density models

K_f	Model		
	Neuber	Molski–Glinka	Macha–Łagoda
	σ_{max}, MPa		
4.62	319	293	305
3.05	287	265	276
2.52	266	245	255

Based on these results it can be concluded that the Neuber model gives the highest stresses and Molski–Glinka model – the lowest values of stresses at the notch root.

Comparing Tables (3) and (4) we may note that the K_t factor is higher than K_f. In the case of a sharp notch ρ = 0.2 mm this difference is more than twice. Therefore, using the analysis of K_t calculated for the sharp notches one should be aware that the value is significantly different from the actual results obtained from the experiment.

CONCLUSIONS

The following conclusions can be drawn, based on the experimental fatigue lives for the tested material: during testing a strong influence of stress concentration on fatigue life was noticed; for different notches different periods of the fatigue cracks were observed; during constant load fatigue testing the weakening of the material and initiation increase in strain was observed; stress values at the notch root for the tested material derived from the Macha–Łagoda model are intermediate compared to other analyzed models.

РЕЗЮМЕ. Подані втомні властивості зразків з подвійними симетричними боковими вирізами (радіуси концентратора від ρ = 0,2 до 10 mm) з сталі FeP04. Для випробувань використовували сервогідравлічний пристрій MTC 809. Втомні випроби виконані за постійного номінального коефіцієнта навантаження (R = 0), амплітуди навантаження 6 kN для радіуса концентратора ρ = 0,2 mm і 7 kN для радіусів ρ = 1,25; 2,5 і 10 mm. Частота навантаження 13...15 Hz. Під час випробувань з постійним втомним навантаженням спостерігали знеміцнювання матеріалу зі збільшенням деформованості.

РЕЗЮМЕ. Представлены усталостные свойства образцов с двойными симметричными боковыми вырезами (радиусы концентратора от ρ = 0,2 до 10 mm) из стали FeP04. Для испытаний использовали сервогидравлическое устройство MTC 809. Усталостные испытания выполнены при постоянном значении номинального коэффициента нагружения (R = 0), амплитуде нагружения 6 kN для радиуса концентратора ρ = 0,2 mm и 7 kN для радиусов ρ = 1,25; 2,5 и 10 mm. Частота нагружения изменялась в пределах от 13 до 15 Hz. Во время испытаний с постоянным усталостным нагружением наблюдалось разупрочнение материала и увеличения деформируемости.

Acknowledgements. Authors are grateful to the scientists Filippo Berto, University of Padova, Department of Management and Engineering, Vicenza, Italy, for the conducting common resarches.

1. *Cavallini M., Di Bartolomeo O., and Iacoviello F.* Fatigue crack propagation damaging micromechanisms in ductile cast irons // Engng. Fract. Mech. – 2008. – **75**. – P. 694–704.
2. *Ding F., Feng M., and Jiang Y.* Modeling of fatigue crack growth from a notch // Int. J. Plasticity – 2007. – **23**. – P. 1167–1188.
3. *Rozumek D.* Influence of the notch radius on changes of the ΔJ parameter under fatigue crack growth rate // J. Theor. and Appl. Mech. – 2009. – **47**. – P. 751–759.
4. *Influence* of the notch (tip) radius on fatigue crack growth rate / D. Rozumek, E. Macha, P. Lazzarin, and G. Meneghetti // Ibid. – 2006. – **44**. – P. 127–137.
5. *Thum A., Petersen C., and Swenson O.* Verformung, Spannung und Kerbwirkung. – VDI, Düsseldorf, 1960. – P. 73–79.
6. *Balytskyi O. I., Kolesnikov V. O., and Kubicki J.* Enhancement of the crack resistance of manganese cast irons // Materials Science – 2005. – **41**, № 1. – P. 67 –73.
7. *Neuber H.* Theory of stress concentration for shear-strained prismatical bodies with arbitrary nonlinear stress-strain law // ASME J. Applied Mech. – 1961. – **28**. – P. 544–550.
8. *Molski K. and Glinka G.* A method of elastic-plastic stress and strain calculation at a notch root // Mat. Sci. and Engng. – 1981. – **50**. – P. 93–100.
9. *Łagoda T. and Macha E.* Multiaxial random fatigue of machine elements and structures, Cyclic energy based multiaxial fatigue criteria to random loading. P. III // Studies and Monographs 104. – TU Opole, 1998. – P. 184 (in Polish).

Received 17.01.2011